

LISA: Pointing Sensor Development Stand

F. G. Dekens, M. Boghosian and A. Abramovici

Jet Propulsion Laboratory, California Institute of Technology, Pasadena, Ca, USA

ABSTRACT

We are developing a pointing sensor as part of the technology development effort for the Laser Interferometer Space Antenna (LISA) mission. The sensor will measure the angle between two beams, by measuring the phase difference in the heterodyne frequency on different sides of the pupil plane. In LISA, one beam would be from the local laser, while the other beam comes from a different spacecraft. The beam coming from the other space craft will have a Doppler shift due to changes in the orbits of the satellites. The phase difference across the aperture will be measured to align the incoming and outgoing beams. We have characterized our pointing noise levels due to electronics over bandwidths of 0.001 to 1 Hz with a heterodyne frequency of 5 MHz. The LISA pointing requirement is on the order of $10 \text{ nrad}/\sqrt{\text{Hz}}$ stability on the sky, with a worst case scenario of $1 \text{ nrad}/\sqrt{\text{Hz}}$. We present our first results, in which we have reached $4 \text{ micro-radians}/\sqrt{\text{Hz}}$ on the detector. This is equivalent to $70 \text{ nrad}/\sqrt{\text{Hz}}$ for LISA.

Keywords: LISA, space interferometry, pointing sensor

1. INTRODUCTION

We are developing a pointing sensor for the LISA^{1,2} mission. This pointing sensor is to be used in order to align the local outgoing beam with the incoming beam from other spacecraft five million kilometers away. Each arm of the interferometer spanning two spacecraft has two of these sensors to keep the interferometric arm aligned, and there are three such arms forming a triangle. The alignment requirement depends on the wavefront quality of the outgoing optics.³ It ranges from 1 to 50 nrad depending on the total aberrations of the outgoing optics. These requirements correspond to aberrations of $\lambda/8$ to $\lambda/100$ RMS, where for LISA the planned wavelength is $1.064 \mu\text{m}$.

Because the spacecrafts are moving with respect to one another, a Doppler shift occurs which can conveniently be used as a heterodyne signal for the pointing sensor. This LISA heterodyne frequency will vary by 15 MHz through the lifespan of the mission. The incoming beam will be combined with a small amount of the outgoing beam using a beam-combiner. The rest of the outgoing beam then goes through an on-axis times-sixty beam expander pointed to the other spacecraft. The same optics take the incoming beam and compresses it by a factor of sixty. Once the beams are combined they go to the pointing sensor's quad-cell.

The challenges for this pointing sensor are the combination of a high frequency heterodyne signal, which does not allow for timing of the zero crossing of the sine wave, and the low frequency drift requirement of order $10 \text{ nano-radians}/\sqrt{\text{Hz}}$ at one milli-Hz.

We start with a brief description of the principle of the sensor. In section 3, we describe the laboratory optical setup, including the source and the different conditions we subject the sensor to. We describe the detector electronics and how we calibrate the sensor in section 4. The following section contains our results. We end with our conclusion in section 6

Further author information: (Send correspondence to F.G.D.)

F.G.D.: E-mail: fdekens@jpl.nasa.gov

M.B.: E-mail: Mary.Boghosian@jpl.nasa.gov

A.A.: E-mail: Alexander.Abramovici@jpl.nasa.gov

2. PRINCIPAL OF THE SENSOR

The pointing sensor consists of four separate heterodyne measurements, each measuring a quadrant of the pupil plane. The pupil is re-imaged on a quadrant cell and the beat frequency is observed in each quadrant. This beat frequency is due to the Doppler shift between the incoming and outgoing beams, which in turn is due to the changing orbits of the three spacecraft, whose relative distances change with time. Although each of the quadrants will detect the same heterodyne frequency, they will have different phases. The phases depend on the tilt between the two beams. By measuring these phases, one can obtain the tip and tilt between the incoming and outgoing beams. The average phase change of all four quadrants contains no tilt information and is thus ignored for this setup.

This proposed technique to measure the beam pointing is similar to the one used by LIGO which reached a sensitivity of 10^{-8} radians.⁴ For this test stand, we care about the particulars of the frequency spectrum and want to verify the resolution of $1 \text{ nrad}/\sqrt{\text{Hz}}$ between 1 and 100 milli-Hz regardless of the heterodyne frequency.

In figure 1, we show a simple illustration of how the pointing sensor works. The average phase, $\bar{\phi}$, over the top half of

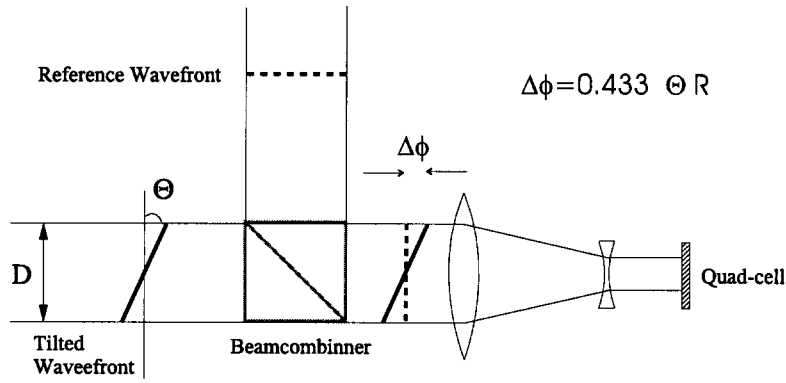


Figure 1. Simple layout of combining a tilted incoming wavefront with a reference wavefront. At the quadrant cell detector, the phase of the beat frequency between the two beams is shifted between the top half and the bottom half of the aperture.

an aperture is the integral of a tilted plane over that half aperture. The phase on the tilted plane is equal to $y\theta$ where y is an axis along the aperture diameter and θ is the angle of the plane. The integral which yields the average phase is

$$\bar{\phi} = \int_{-R}^R \int_0^{\sqrt{R^2-x^2}} y \theta \, dy \, dx, \quad (1)$$

where R is the input aperture radius and x, y are coordinates in the aperture plane. Evaluating the integral gives

$$\bar{\phi} = \frac{4}{3\pi} \theta R. \quad (2)$$

The fraction out front evaluates to 0.424. Note that had the integral been evaluated over a square aperture, the factor out front would simple be one half. Also note that compressing the beam does not change this result. As the beam is compressed, the radius decreases, the tilt of the wavefront increases proportionally and the average phase delay stays the same.

For LISA, where we take the input aperture diameter, D , to be 30 cm, the phase difference for the top half of the aperture of a plane with one nano-radian tilt is then 0.064 nm. This means that in order to meet the LISA pointing measurement, we need four interferometric type measurements of each $0.064 \text{ nm}/\sqrt{\text{Hz}}$ sensitivity over the frequency range from 1 to 100 milli-Hz.

3. OPTICAL SETUP — SOURCE

We begin with the light source of the test stand. This is meant to mimic the Doppler shift that occurs between the local and incoming laser beams. In particular, it needs to have variable heterodyne frequencies. Of less importance is the actual wavelength of the light. For ease of use, we are currently using a 7 milli-Watt He Ne laser, which we split through two IntraAction Corp. acousto-optic modulators (AOM). The two AOM's are driven at frequencies of 40 and 45 MHz. The latter frequency can be varied from 10 kHz to 80 MHz in 10 kHz increments. Each beam is then coupled to a single mode fiber. A schematic layout is shown in figure 2. The fiber outputs can be combined using either a fiber beam combiner or

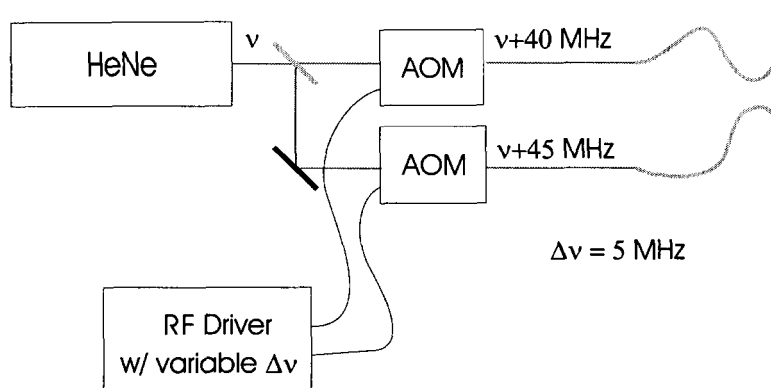


Figure 2. Schematic layout of the Heterodyne source.

a beam combining cube. In the latter case, the output of each fiber is collimated to a 5 mm beam and pointed such that they combine on a half inch beam combining cube. The resultant combined beam then goes to the quad-cell detector. If the two source beams are combined using the fiber beam combiner, one output fiber is collimated and goes directly to the quadrant cell. We remove the half inch beam combiner cube in that case.

The fiber beam coming method gives us a way of ideally combining the two interfering wavefronts without having tilt between them. This allows us to test the sensor at a zero tilt condition without introducing mechanical tilt drifts due to the mounts or drift due to the turbulence inside the enclosure. When we do use the beam combining cube, we can intentionally introduce a tilt, which we then measure using the sensor. This allows us to calibrate the sensor using a known mechanical tilt.

One final optical setup is to replace the entire source with a blinking LED. This eliminates possible source drifts and gives us a type of background measurement. The LED is then driven by a function generator whose output is 5 MHz. The amplitude is adjusted such that the output voltage of the quad-cell is the same as when the heterodyne laser source is illuminating the quad-cell. The LED is placed directly in front of the quad-cell.

4. DETECTOR SETUP

The sensing element itself is a large area quad-cell detector made by Pacific Silicone Sensor, Inc., model PSS-QP50-6-5M. It has an active area of 50 mm². Each quadrant has an AD827 based amplifier circuit whose bandwidth ranges from 20 kHz to 20 MHz.

The typical output of a quadrant amplifier is 40 milli-Volts peak to peak when the quad-cell is illuminated by our heterodyne laser source. This is currently amplified to 400 millivolts by a Mini-Circuits ZFL-500 RF amplifier. For now, we are only using two quadrants, once we have met our pointing requirement in one dimension, we will duplicate the electronics for all four quadrants so that we can monitor both tip and tilt and have one redundant quadrant for self consistency checking.

A schematic layout is shown in figure 3. In order to obtain the phase difference between the two signals using an RF mixer, we need one of the signals to be delayed by 90 degrees. Until recently, this was accomplished using a 9.6 meter long BNC cable. This causes 86 degrees of phase delay on the 5 MHz signal we are currently using. This method work

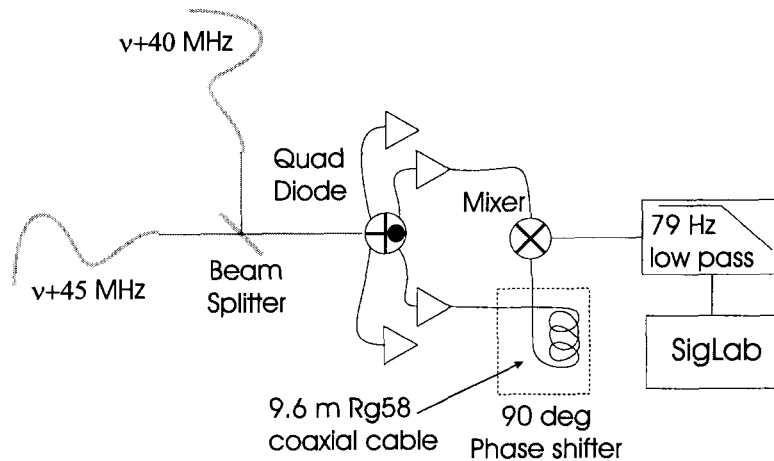


Figure 3. Schematic layout of the sensor electronics.

well at just that frequency, but introduces an undesired frequency dependence. We are currently developing a fixed ninety degree phase shifter that produces less than a few percent of phase over the possible heterodyne frequency range of LISA. The last few percent could potentially be calibrated if it is repeatable. The mixer we currently use is a ZAD-8 Mini Circuits component, which has an acceptable range of 0.0005 to 10 MHz. The output of the mixer is low pass filtered by a 79 Hz RC filter. Finally the output of that is recorded using a Spectral Dynamics SigLab at 5 Hz for 3 to 16 hours. In order to convert the measured voltage to angle on the detector, we obtained an empirical calibration. This is described next.

4.1. Calibration

In order to calibrate the sensor, we use an 600A-2 Newport optical mount which allows us to tilt one of the beams by small amounts using a micrometer. Figure 4 shows the calibration data for the sensor. The X-axis is the mechanical tilt measured from dividing the micrometer reading by the mechanical level arm of 87 mm of the mount. For each angle, the resultant filtered mixer output was recorded; these are the Xs in the figure. The slope of the linear part near zero voltage was used as the calibration. Note that the strongest signal and 90 degree phase was verified to happen at that zero crossing. The fitted slope is -3.14 milli-Volts per micro-radian of wavefront tilt, where we have multiplied by an additional factor of 2 to convert from mechanical tilt of the mirror to wavefront tilt. The sign is arbitrary because either quadrant can be fed into the local oscillator side of the mixer. On either side of the linear region of the curve, the signal degrades because the amplitude of the heterodyne interference signal decreases, due to the tilt and beam walk errors becoming too large.

4.2. Electronics Background

We measured the background voltages at 5 Hz for 3 to 16 hours. The background voltage levels were converted to background levels of the detector in angle using the calibration from section 4.1. We also included an additional factor of 60 to convert from for angle at the detector to angle on the sky. There are three different backgrounds, whose power spectral densities (PSD) are shown in figure 5. Each of the curves represents measurements which include more and more of the test setup. The first measurement is simply the data acquisition system with a 50 Ohm terminator directly on the input to show that it is adequate to meet our requirement of 1 nano-radian. The second measurement, “function generator”, is a 5 MHz sine wave from a function generator what is split and connects to the RF amplifiers, then the long cable that we use as the 90 degree phase shifter, the mixer and the low pass filter. The “blinking LED” measurement is taken by placing an LED, which blinks at 5 MHz, in front of the quad-cell. Two quadrants of the quad-cell are then connected to the RF amplifiers. Past that, the electronics are the same as in the previous measurement. The LED intensity is adjusted to yield the same voltage levels out of the quad-cell as when the heterodyne laser illuminates the it.

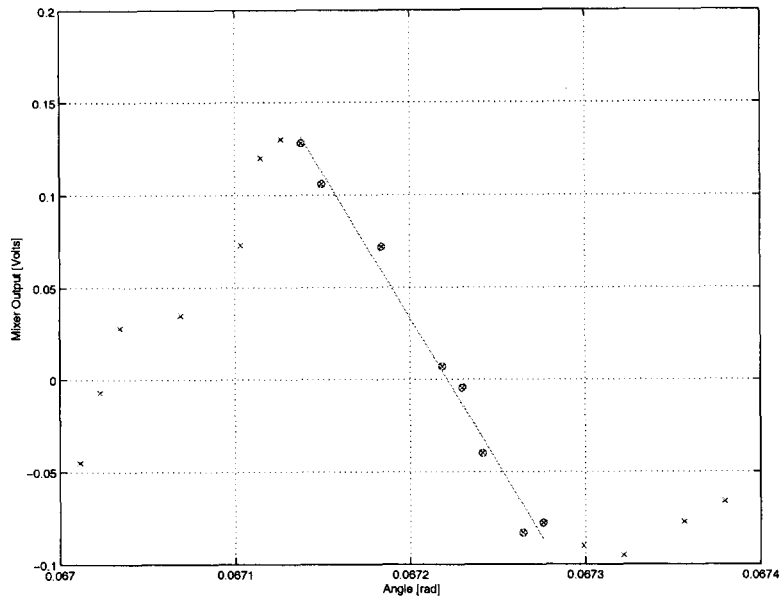


Figure 4. This is the output voltage vs. measured mechanical tilt angle in order to calibrate the pointing sensor. The Xs are the measurements. The circled Xs are the data points to which the line has been fitted. The slope of the line is -1.57 milli-Volts per micro-radian of mechanical tilt.

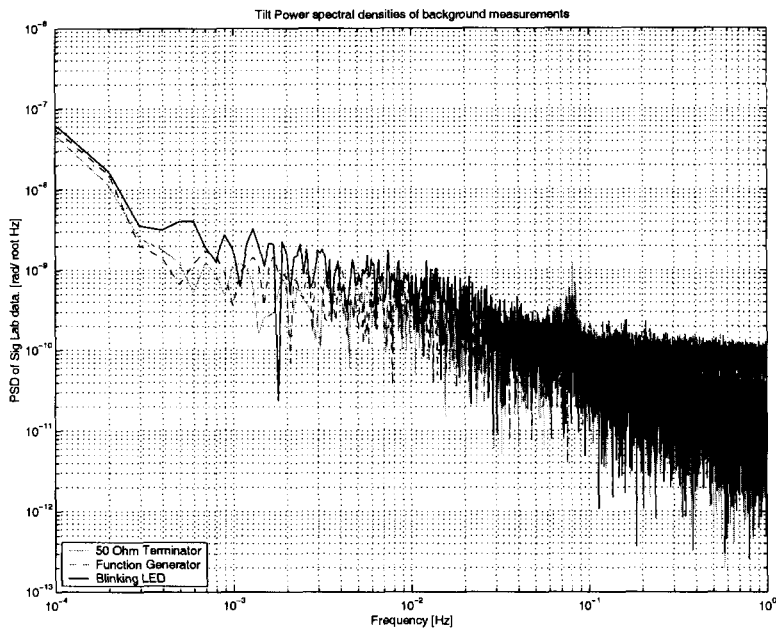


Figure 5. These are the power spectral densities of background tests.

5. RESULTS

We now compare data runs with two different beam combiners. The two beam combiners are a fiber beam combiner and an in-air cube beam combiner. Their power spectral densities are shown in figure 6. The measurement run with a blinking LED was included for reference. The fiber beam combiner performs better than the in-air cube beam combiner; however, it is still significantly worse than the electronics limitation as measured by the LED. The difference in results between the

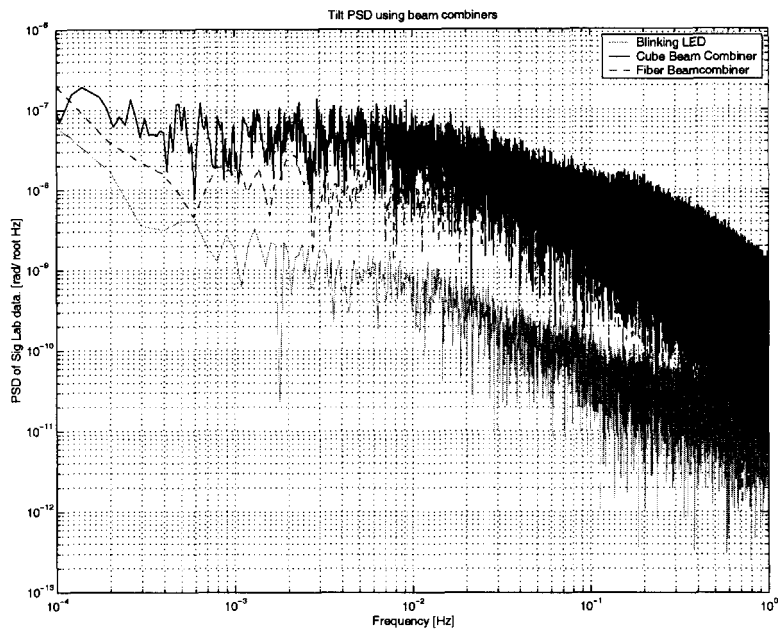


Figure 6. These are the power spectral densities of background tests.

fiber beam combiner and the cube beam combiner is due to a combination of mechanical, thermal and turbulence drifts. These measurements were made after enclosed the setup in a small one-inch thick gatterboard to minimize the turbulence and thermal drifts.

Our current limitation between the fiber beam combiner and the LED cases, is believed to be due to light intensity and heterodyne frequency variations of the beam. Figure 7 shows peaks in the power spectral densities by intentionally modulating the source signals. In each case, the modulating frequency was 0.5 Hz and sinusoidal. In the “Splitter: 20% ampl. mod.” case, the function generator signal amplitude was modulated by twenty percent. The signal is split using an RF splitter and both signals then go to the RF amplifiers. In the “LED: 20% ampl. mod.” curve, the function generator output drives the LED which is placed directly in front of the quad-cell. Again the maximum amplitude was adjusted to be the same as when the heterodyne laser source is illuminating the quad-cell. Note that the peak of the LED case is smaller. This is probably due to the LED not being linear and although it’s driving amplitude was varied by twenty percent, the actual amplitude did not vary by as much. In the last curve, the 5 MHz sine wave was frequency modulated by 1 kHz. In each case, several hour long data runs were taken and the x-axis in the figure was set to just show the peak. There is a slight offset in frequency between the amplitude and frequency modulations. This is because the frequency generator was capable of modulating the frequency on it’s own; however, to perform the amplitude modulation that we needed, a second function generator had to be used. The second function generator’s amplitude was fed into the first’s external input. The two function generators were not synchronized to the same clock at the time.

The frequency modulation is expected since for now we are using a large cable as our 90 degree frequency shifter. We will continue to track this effect as we switch to a frequency independent phase shifter. The driving requirement for the phase shifter development will be mitigate this heterodyne frequency dependent phase effect.

The amplitude sensitivity is also undesired. However, they are likely to be present in both the mission and in the lab setup. In the latter case, the largest amplitude changes come from the polarization drifts in the fibers. As the polarization changes, the intensity of the interfering light changes and hence so does the quad-cell output. In order to be less susceptible to this, we will switch to different RF amplifiers whose output signals are larger saturate the diodes of the mixer. If that still limits us, we may have to modify the RF amplifiers to have a variable gain with a control loop to keep the output amplitude constant.

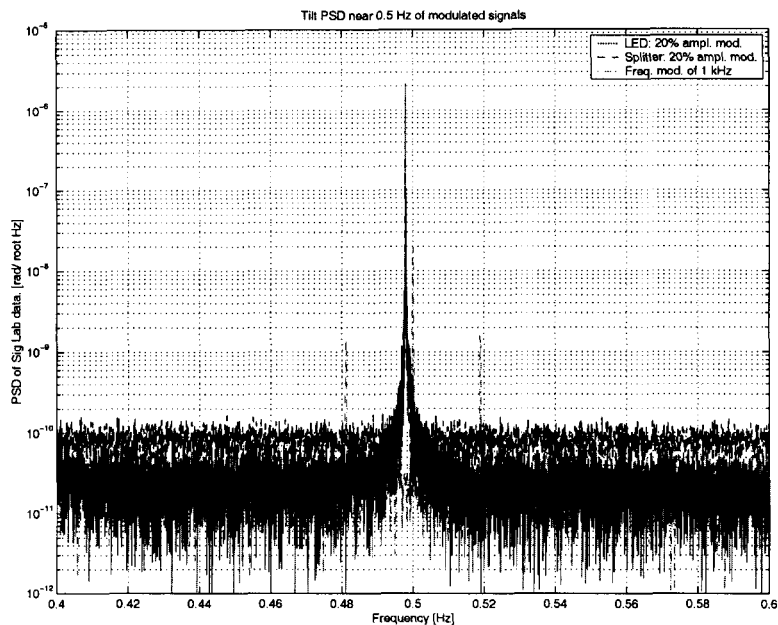


Figure 7. These are the power spectral densities of peaks due to amplitude and frequency modulations of the signal.

6. CONCLUSION

We have build the source and our first iteration of detector for the LISA pointing sensor test stand. This setup is adequate to test further electronic developments such as a heterodyne-frequency independent 90 degree phase shifter and amplitude independent methods of combining the signals.

The electronics background levels are a factor of two above the LISA worst case pointing requirement of $1 \text{ nrad}/\sqrt{\text{Hz}}$. Our current tilt background level at 1 milli-Hz is $4 \text{ micro-radians}/\sqrt{\text{Hz}}$ at the detector or $70 \text{ nrad}/\sqrt{\text{Hz}}$ on the sky for LISA, assuming a factor of 60 in the compression optics. We have identified our limitations due to amplitude and heterodyne frequency drifts and have described our path towards meeting the LISA pointing requirement.

ACKNOWLEDGMENTS

The authors thank Jake Chapsky, Danial Saddock, Jeff Sneider and Meng for their valuable discussions and help. The research described in this paper was carried out at the Jet Propulsion Laboratory, California Institute of Technology, under a contract with the National Aeronautics and Space Administration.

REFERENCES

1. W. M. Folkner, P. L. Bender, and R. T. Stebbins, "Report on measured image motion at the keck telescope," JPL Publication 97-16, Jet Propulsion Laboratory, California Institute of Technology, 4800 Oak Grove Dr., Pasadena, Ca 91109, Feb. 1999.
2. L. S. T. 2000, "Laser interferometric space antenna: a cornerstone mission for the observation of gravitational waves," Tech. Rep. ESA-SCI 11, European Space Agency, 2000.
3. M. V. Papalexandris and E. Waluschka, "Numerical phase front propagation for a large-baseline space interferometer," *submitted to Optical Engineering*, 2002.
4. P. Fritschel, N. Mavalvala, D. Shoemaker, D. Sigg, M. Zucker, and G. Gonzalaz, "Alignment of an interferometric gravitational wave detector," *Applied Optics* **37**, pp. 6734–47, Oct. 1998.